Seismically induced rock slope failures resulting from topographic amplification of strong ground motions: The case of Pacoima Canyon, California

Sergio A. Sepúlveda [a,b,*], William Murphy [a], Randall W. Jibson [c], David N. Petley [d]

[a] *School of Earth and Environment, University of Leeds, Leeds LS2 9JT, UK*
[b] *Departamento de Geología, Universidad de Chile, Casilla 13518- Correo 21, Santiago, Chile*
[c] *U.S. Geological Survey, Box 25046, MS966, Denver Federal Center, Denver CO 80225, USA*
[d] *Department of Geography, University of Durham, Durham DH1 3LE, UK*

Abstract

The 1994 Northridge earthquake (M_w=6.7) triggered extensive rock slope failures in Pacoima Canyon, immediately north of Los Angeles, California. Pacoima Canyon is a narrow and steep canyon incised in gneissic and granitic rocks. Peak accelerations of nearly 1.6 g were recorded at a ridge that forms the left abutment of Pacoima Dam; peak accelerations at the bottom of the canyon were less than 0.5 g, suggesting the occurrence of topographic amplification. Topographic effects have been previously suggested to explain similarly high ground motions at the site during the 1971 (M_w=6.7) San Fernando earthquake. Furthermore, high landslide concentrations observed in the area have been attributed to unusually strong ground motions rather than higher susceptibility to sliding compared with nearby zones. We conducted field investigations and slope stability back-analyses to confirm the impact of topographic amplification on the triggering of landslides during the 1994 earthquake. Our results suggest that the observed extensive rock sliding and falling would have not been possible under unamplified seismic conditions, which would have generated a significantly lower number of areas affected by landslides. In contrast, modelling slope stability using amplified ground shaking predicts slope failure distributions matching what occurred in 1994. This observation confirms a significant role for topographic amplification on the triggering of landslides at the site, and emphasises the need to select carefully the inputs for seismic slope stability analyses.

Keywords: Landslides; Earthquakes; Site effects; Slope stability

1. Introduction

Extensive rock slope failures were triggered at Pacoima Canyon, southern California, during the 1994 Northridge earthquake (M_w=6.7). Pacoima Can-

* Corresponding author. Departamento de Geología, Universidad de Chile, Casilla 13518- Correo 21, Santiago, Chile. Fax: +56 2 696 3050.
E-mail address: sesepulv@ing.uchile.cl (S.A. Sepúlveda).

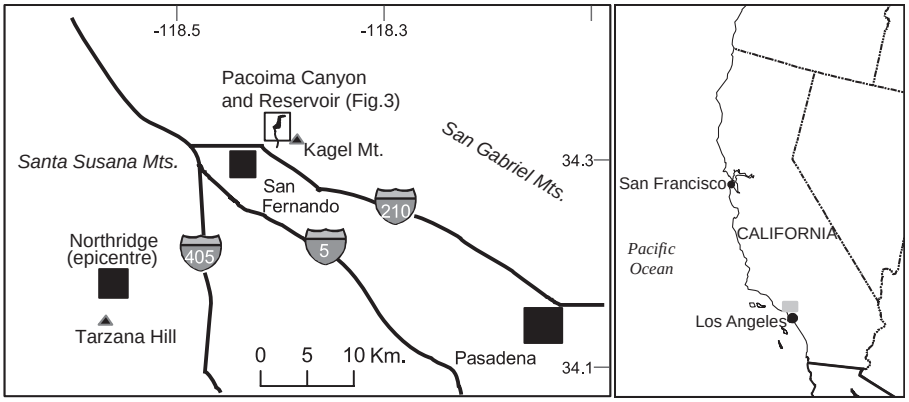

Fig. 1. Location map of Pacoima Canyon and other sites near Los Angeles mentioned in the text. The grey box in the right map shows the extension of the left map.

yon is located in the San Gabriel Mountains, on the north border of the Los Angeles metropolitan area, near the city of San Fernando, about 20 km northeast from the 1994 epicentre (Fig. 1). In the lower part of the canyon, Pacoima Dam (a concrete arch dam completed in 1929) impounds a reservoir used for water storage and flood control (Fig. 2).

A peak ground acceleration (PGA) of 1.58 g was recorded during the 1994 earthquake on the ridge that forms the left dam abutment. Accelerations in surrounding areas and at the bottom of the canyon, however, were generally less than 0.50 g. This localized disparity in shaking levels suggests the occurrence of topographic amplification of the ground motion, an effect caused by the interaction of the incoming seismic waves with certain geomorphic features such as steep slopes in areas of strong topographic relief. The effect generally results in larger amplitudes of the ground motion toward ridge crests (Geli et al., 1988). While this topographic effect has been found to be of secondary importance compared to other site amplification effects in soil slopes (Ashford et al., 1997), it may be a significant source of site amplification on rock slopes and therefore an important factor controlling their stability during strong earthquakes.

At the same location where the high peak acceleration was recorded in 1994, a peak acceleration of

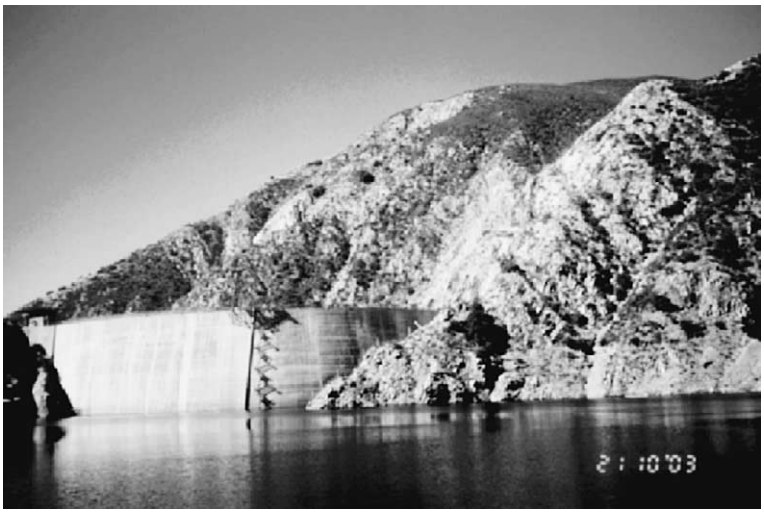

Fig. 2. Pacoima dam and reservoir, and rock mass of the right dam abutment.

Table 1
Peak accelerations recorded at Pacoima Canyon during the 1971 and 1994 earthquakes

Earthquake	Station	Location	Component of movement (azimuth)	Peak acceleration (g)
1971 San Fernando	PCD	Left dam abutment	164°	1.23
			254°	1.16
			Vertical	0.70
1994 Northridge	PUL	Left dam abutment	104°	1.58
			194°	1.28
			Vertical	1.23
1994 Northridge	PAC	Canyon bed	175°	0.42
			265°	0.43
			Vertical	0.19

1.23 g was recorded during the 1971 San Fernando (M_w=6.7) earthquake (PEER, 2000; Table 1). Several authors (Boore, 1972, 1973; Bouchon, 1973; Wong and Jennings, 1975) have explained the high accelerations recorded at the ridge as a consequence of topographic amplification. A later study by Anooshehpoor and Brune (1989) based in a laboratory model, did not confirm the strong influence of topographic effects but showed that strong motion amplifications at the site depend on both the direction of approach and the angle of incidence of the seismic waves. These factors have been recognised as important for the occurrence of topographic amplification by Ashford and Sitar (1997).

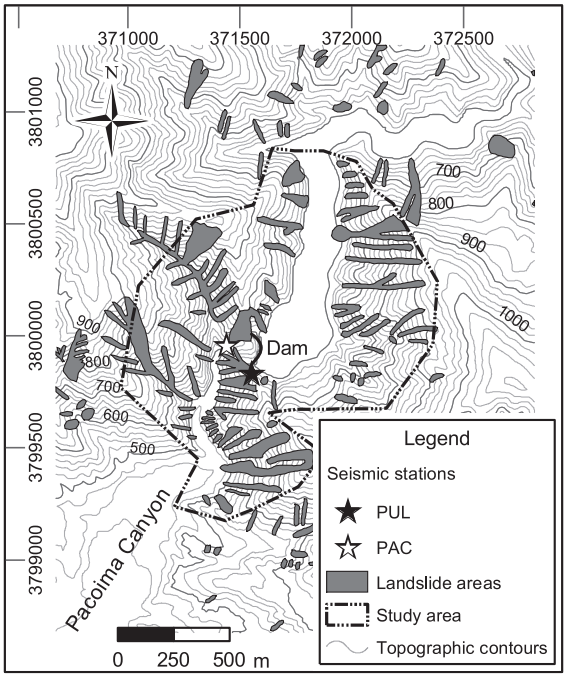

Fig. 3. Topographic map of Pacoima Canyon and reservoir with indication of the area of study and zones strongly affected by landsliding (after Harp and Jibson, 1996) during the 1994 earthquake, and location of seismic stations that recorded the strong motions at the site. (Topographic base source: USGS).

High landslide concentrations observed in the area following both earthquakes could not be explained by higher susceptibility to sliding compared with nearby zones, and therefore have been attributed to amplified strong motions (Harp and Jibson, 2002). We conducted additional field investigations and slope stability back-analyses to confirm the effects of topographic amplification on the triggering of landslides during the 1994 earthquake. The area of study for the analyses includes the canyon from its southern entrance up to the dam and the reservoir shores in the southern half of the reservoir, where the valley has a north–south orientation (Fig. 3). The reservoir area was accessed by boat, while the canyon downstream from the dam (Fig. 4) was accessed by foot.

2. Geology and geomorphology

The regional geology of the study area (Yerkes, 1996) is dominated by a Cretaceous intrusive body composed of coarse-grained granitic rocks ranging from quartz diorite to granite but mainly consisting of granodiorite. Gneissic facies are present near contacts with older rocks, typically Mesozoic diorite gneiss that crop out around the reservoir. Our field observations revealed that granitic rocks form most of the north and west shores of Pacoima reservoir, part of the northeast shore where the canyon has an east–west orientation, and the southern entrance of

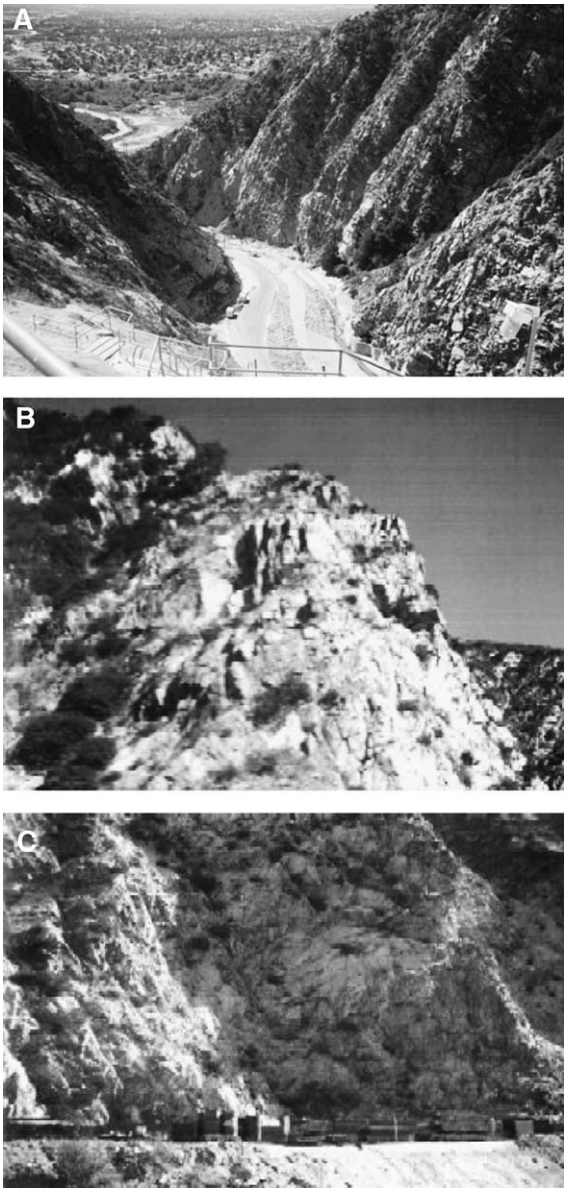

Fig. 4. (A) View of Pacoima Canyon downstream from the dam. In the background, San Fernando Valley. (B) Upper part of a slope prone to rock falling. (C) Example of planar sliding failures caused by unfavourable joints dipping out of the slope.

the canyon (Fig. 5). Gneiss forms most of the east shore of the reservoir, the left abutment of the dam, and the east bank of the canyon immediately downstream from the dam. Most of the gneissic outcrops around the dam are currently supported by shotcrete. The right dam abutment and the west canyon bank downstream from the dam are composed of a mixture of granitic and gneissic facies (Fig. 5). Local faults control the orientation of lateral gullies and some of the contacts between granitic and gneissic bodies. The water table is assumed to be close to the elevation of the reservoir. Harp and Jibson (2002) described the condition of the rock slopes during the 1994 earthquake as "extremely dry", therefore the slopes of the canyon will be assumed to be dry for the analyses below.

The canyon geomorphology is characterised by strong topographic relief (Fig. 3), particularly the canyon section downstream from the dam, where the canyon bottom is no more than about 50 m wide and is bounded by 200 m high rock walls of 45°–65° (Fig. 4). The slopes around the reservoir are 200–300 m high and have slope angles generally between 35° and 55°. Tributary canyons have slopes of 40°–55°.

3. The 1994 Northridge earthquake and associated landslides

On 17 January 1994 a M_w=6.7 earthquake shook the Los Angeles area. The epicentre was at the city of Northridge, about 20 km southwest of Pacoima Dam. The focal distance was about 27 km (Harp and Jibson, 1996; see Fig. 1). The rupture occurred on a blind thrust fault. The fault plane has a strike of 122° and a dip of 42° to the southwest, with a along-strike width of 14 km and a 19.5 km down-dip width. The depth of the top of the rupture plane was 7 km from the ground surface (Chang et al., 1996). Peak free-field accelerations varied but were as high as 0.90 g on soil and 0.83 g on rock (Chang et al., 1996). Anomalously high accelerations were recorded at Tarzana Hill, located 6 km south of the epicentre (Fig. 1) and Pacoima Dam. The 1.78 g acceleration recorded at Tarzana was attributed to a combination of topographic and soil amplification (resonance) effects (e.g. Spudich et al., 1996; Vahdani and Wikstrom, 2002). The 1.58 g acceleration at Pacoima Dam has been attributed to topographic amplification (Chang et al., 1996; Harp and Jibson, 2002), similar to the situation in the 1971 earthquake.

During the mainshock, the instrument located on the left dam abutment (station PUL, Fig. 3) recorded a peak horizontal acceleration of 1.58 g and a peak

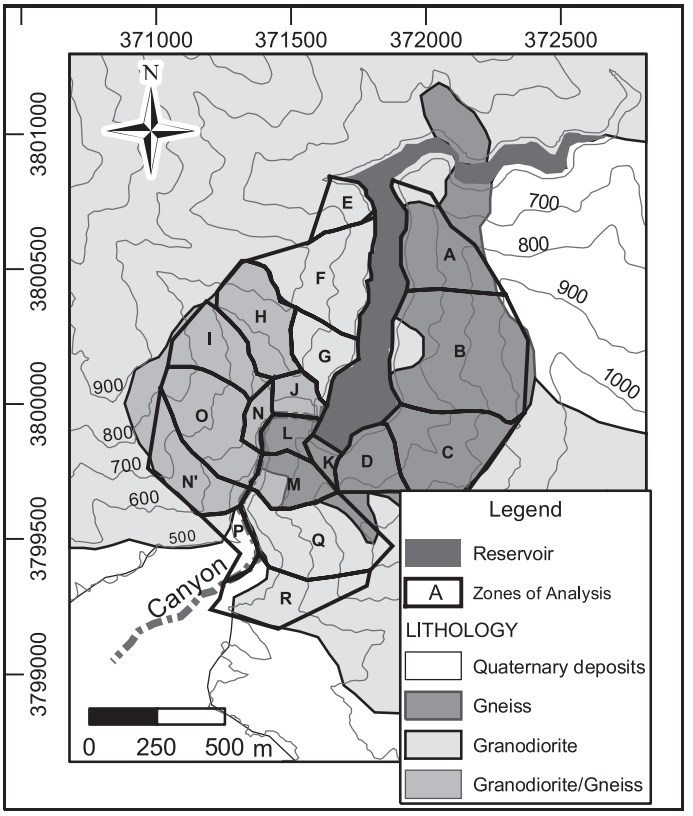

Fig. 5. Geological map of the Pacoima Canyon area (modified from Yerkes, 1996), and subdivision of the study area in zones of geomorphological and geological similarity used for the slope stability analyses. Zone N` has the same mean orientation and slope angle that zone N and therefore for the analyses they are grouped as one.

vertical acceleration of over 1.00 g (Table 1). The total duration of the mainshock at this station was about 13 s. The case for topographic amplification to explain the high accelerations is supported by records from a station at the bottom of the canyon a few tens of metres downstream from the dam (station PAC, Fig. 3). The horizontal distance between the stations is about 200 m, and the difference in elevation is about 100 m. The station PAC recorded a peak ground acceleration of 0.43 g (Table 1). The total duration was about 10 s. This ground motion is similar to those recorded by other nearby stations and is consistent with the ground motion attenuation pattern for free-field stations in the region (Chang et al., 1996). Furthermore, the closest seismic station outside the canyon, located at Kagel Mountain, less than 2 km east of the dam (Fig. 1), recorded a PGA of 0.44 g. Therefore, it is assumed that possible deamplification effects, sometimes observed at the bottom of canyons, were not significant and the PAC record can be assumed as representative of shaking unaffected by amplification or deamplification by comparison with the PUL record.

The Northridge earthquake triggered more than 11,000 landslides over an area of 10,000 km^2 (Harp and Jibson, 1996). The landslides were mainly concentrated in the Santa Susana Mountains, west of San Gabriel Mountains (Fig. 1). Here, thousands of shallow (1 to 5 m thick), highly disrupted slides and falls in weakly cemented clastic sediments were triggered, together with dozens of more coherent rotational slumps and block slumps. More detailed description of these landslides can be found in Harp and Jibson (1996). Landslides were much more sparsely scattered in the more competent rocks of San Gabriel Mountains, with the notable exception of

Pacoima Canyon, where the concentration of landslides was as high as in Santa Susana Mountains (Harp and Jibson, 2002). The landslides in Pacoima Canyon were mainly rock block slides and falls, or commonly a combination of both, *i.e.* block sliding that derived in falling from the higher parts of the slopes. The block size varies from some decimetres to several metres of diameter, formed by pre-existent joints in the granitic and gneissic rocks (Fig. 4). Details of the jointing pattern and failure modes are presented in the following section.

Harp and Jibson (2002) used a modified version of the rock mass quality (Q) classification system (Harp and Noble, 1993) to conduct a comparative study of the susceptibility to failure of rock masses in areas around Pacoima Canyon that experienced far fewer landslides in 1994 than did Pacoima Canyon. They found that the rock mass quality of the slopes of Pacoima Canyon downstream from the dam is similar to that of slopes of comparable steepness and geology at four adjacent areas. The 1994 landslides were triggered in dry conditions; therefore the higher density of failures could not be associated to differential groundwater conditions between the different areas. They concluded that the higher landslide density at Pacoima Canyon was most likely caused by topographic amplification.

4. Analysis of the slope failures

4.1. Landslide distribution and kinematic susceptibility to sliding

We assessed the slope stability under shaking conditions during the 1994 earthquake within the study area. The areas affected by landsliding in the canyon (Harp and Jibson, 1996) are shown in Fig. 3. The principal observed type of failure were wedge and planar failures (Fig. 4), which in many cases derived in rock falls. Detailed analyses of specific failures were impossible because of access limitations to the upper parts of the slopes where most failures occurred. Furthermore, the large number of block slides makes the individual study of all the failures impractical. Therefore, for purpose of the analyses, the slopes were grouped into 18 zones of similar geology, slope orientation, and slope angle (Fig. 5). Zones A to K surround the reservoir, while zones L to R represent slopes of the lower canyon and a limited number of subsidiary canyons downstream from the dam. Practically every zone produced landslides in 1994, although landslide densities in zones C, D, F and K were low.

Field observations revealed that discontinuity orientation was an important control on slope instability, especially in the canyon area immediately downstream from the dam. Further, the left dam abutment shows evidence of previous instability due to block sliding associated with water pressure increases caused by intense rainfall in 1938. The slopes that failed during that event were found to be kinematically prone to block sliding (Hatzor and Goodman, 1997).

For the determination of potential slip planes, we measured the orientation of local joint sets using a combination of scanline surveys and measurements of infrequent joints identified as forming slip surfaces. Principal joint set orientations are shown in Fig. 6 and detailed in Tables 2 and 3. The local joint sets were compared with mean slope orientation and slope angles in the upper, steeper parts of the slopes, where most failures were triggered. The kinematic susceptibility for planar, wedge and toppling failures was determined following the methods outlined by Hoek and Bray (1981) to identify the potential failure modes for both rock slides and falls.

The landslide density distribution demonstrates a relationship with the kinematic susceptibility for each zone. For example, zones A, H, K, L, Q and R were found to be very prone to block sliding, while zones B, D, F and I present low kinematic susceptibility, which generally coincides with high and low landslide densities for the respective zones. This confirms the field observations that suggest that discontinuities strongly influence the distribution of landslides. The slopes in the northern area above the dam have medium to high susceptibility to block sliding by planar and wedge failures. Closer to the dam the susceptibility is low, as was the landslide incidence in that area. The left abutment has high susceptibility for a combination of toppling and wedge failures, while the right abutment is less susceptible, concurring with the analyses done by Hatzor and Goodman (1997). Downstream from the dam, the slopes on the

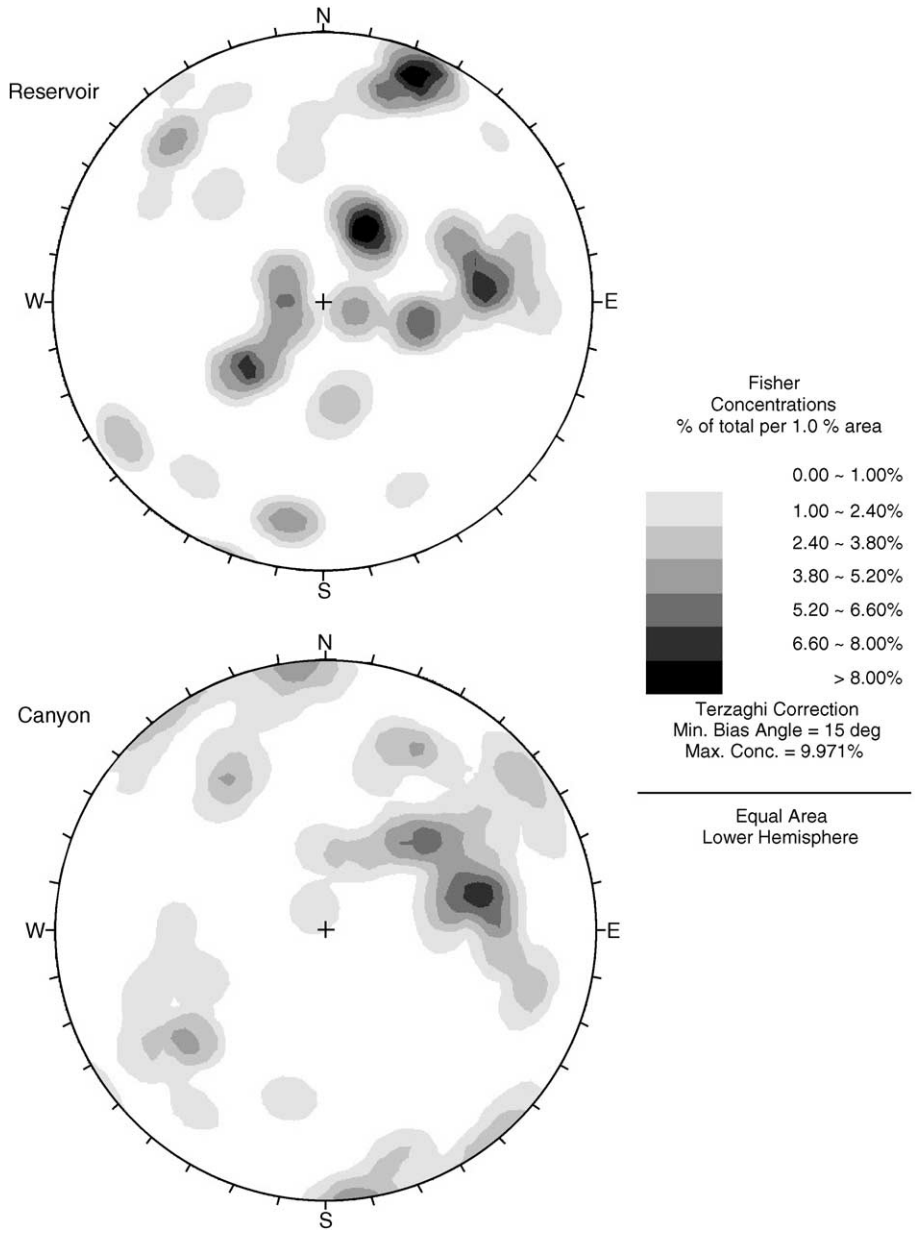

Fig. 6. Stereonets showing pole concentration of joints around Pacoima reservoir and in the canyon downstream from the dam. Principal joint sets defined from these data are shown in Tables 2 and 3.

east bank have a high potential for planar failures and a lower potential for wedge failures, which agrees with the field observations of failures. The stability conditions of the west bank and lateral canyons, by contrast, are mostly dominated by wedge failures.

4.2. Pseudostatic back-analyses

The stability of slopes representative (by slope orientation and angle) of each of the defined zones during the Northridge earthquake was analysed using planar sliding and wedge failure pseudostatic

Table 2
Principal joint sets around Pacoima reservoir

Joint set	Strike	Dip
R1	111°	77°S
R2	121°	26°S
R3	169°	52°W
R4	013°	22°W
R5	141°	24°E
R6	047°	70°S
R7	099°	71°N

Data shown in Fig. 6.

back-analyses. Horizontal and vertical accelerations from seismic records of both PAC and PUL seismic stations were used to allow comparison of the slope stability under normal and topographically amplified strong motions, respectively. Pseudostatic accelerations equal to one half of the peak ground accelerations were used as recommended by Kramer (1996). This approach has found to give consistent results for analysis of strong rock slopes during strong earthquakes (Sepúlveda et al., 2005). Analyses assumed dry slopes corresponding with the conditions reported at the time of the earthquake (Harp and Jibson, 2002). Zone I was not analysed because it showed only low susceptibility to toppling failure.

The strength of rock joints was estimated using the method of Barton (1976). In this approach, an 'equivalent' friction angle (ϕ_{eq}) to be used in a Mohr-Coulomb failure criterion (with zero cohesion) is defined as:

$$\phi_{eq} = \mathrm{JRC}\log(\mathrm{JCS}/\sigma_n) + \phi_b \quad (1)$$

where σ_n is the normal stress; ϕ_b is the basic friction angle of the joint material; JRC is the joint roughness coefficient, estimated from comparison of joint profiles with charts; and JCS is the joint compressive strength, which can be calculated from Schmidt hammer tests on the joint wall. Field measurements of JCS and JRC were used. The compression strength of the rocks, particularly the gneissic facies, is highly variable. This variability of strength was taken into account by using a sub-classification of the gneissic rocks based on local measurements (Table 4). Although Barton's method was developed for static strength conditions, some roughness coefficients were estimated from sliding surfaces that may have suffered shearing of the asperities. Thus, the resultant strength would represent at least partially dynamic strength conditions. Following the recommendations of Barton (1976), strength values derived from very low normal stress were discounted, as they tend to be unrealistically high. Results are shown in Table 4.

Pseudostatic limit equilibrium analyses were performed for the different planar and wedge potential failures indicated by kinematic analyses for each zone, using analytical formulae proposed by Hoek and Bray (1981). To incorporate the uncertainty associated to the analyses, means and standard deviations of pseudostatic factors of safety were calculated using the Latin Hypercube sampling technique with the @Risk add-in for Excel (Palisade Corporation, 2002). Due to insufficient data to quantify the probability distribution of the geotechnical inputs for stability analyses, we assumed all parameters had truncated normal distributions, following the guidelines of Hoek (2000). Standard deviations of the parameters were estimated based on observed variations in the field, while the truncation was based on extreme possible values. Thus, the equivalent friction angle for the correspondent lithology reported in Table 4 was used as the

Table 3
Principal joint sets at Pacoima Canyon, downstream from the reservoir

Joint set	Strike	Dip
C1	083°	87°S
C2	056°	56°E
C3	050°	89°W
C4	156°	44°W
C5	116°	64°S
C6	143°	61°E

Data shown in Fig. 6.

Table 4
Data and results for rock joint strength calculations for the Pacoima Canyon site

Rock type	Basic friction angle	JCS (MPa)	JRC	ϕ_{eq}
"Weak" gneiss	26°	21	8	37°
"Average" gneiss	26°	59	9	42°
"Strong" gneiss	26°	97	10	46°
Granodiorite	31°	105	12	54°

Basic friction angles for dry joints after Barton (1976).

mean value, with standard deviations of 5°, which imply that 68% of the values will be in a range of 10° with centre in the mean. The friction angle distribution was truncated by a minimum value of 20° and a maximum of 70° arbitrarily chosen to represent extreme cases of very smooth and very rough surfaces. Similarly, slip angles were allowed to vary based on field observations. As expected, mean values are practically equal to deterministic factors of safety. The minimum factors of safety obtained for each zone considering all possible failures are presented in Fig. 7. In zones where both planar and wedge failures were analysed, planar surfaces had the lowest factors of safety.

The results show that if the mean values of factors of safety for the base (i.e. unamplified) strong motion (PAC record) are considered, less than half the areas would have suffered failure (factor of safety below 1.0), while the rest would have remained stable. In contrast, when the amplified strong motion is used, all zones showed instability. In general, areas that produced less landsliding, mostly around the reservoir, had higher pseudostatic factors of safety.

The critical acceleration for sliding (Wilson and Keefer, 1985) of potential planar and wedge failures was also calculated. The critical acceleration (A_c, parallel to slip direction) is simply the threshold ground acceleration that must be exceeded for a landslide block to begin moving downslope, defined as:

$$A_c = (F - 1)g\sin\theta \quad (2)$$

where F is the static factor of safety, g is the acceleration of gravity and θ is the inclination of the sliding surface. If the peak acceleration exceeds the critical acceleration, downslope movement will occur. Estimated critical accelerations (Fig. 8) show a pattern similar to that of the pseudostatic factors of safety: for unamplified ground motions, less than half the areas have PGAs greater than the mean critical accelerations; for amplified ground motions, however, all the areas have PGAs exceeding the critical accelerations.

Figs. 7 and 8 show that levels of uncertainty, represented by standard deviations, are significant and should be considered during interpretation. As a means of testing the reliability of assessments, we calculated the probabilities of factors of safety being below 1.0, indicative of failure, by the calculation of cumulative distribution functions of the factors of safety using @Risk. The analyses return very high probabilities (mostly over 95%) for sliding under the amplified conditions recorded at station PUL. However, mixed results were obtained from analyses using unamplified conditions, represented by station PAC: maximum probabilities of failure (among different possible failure modes) were below 10% for five

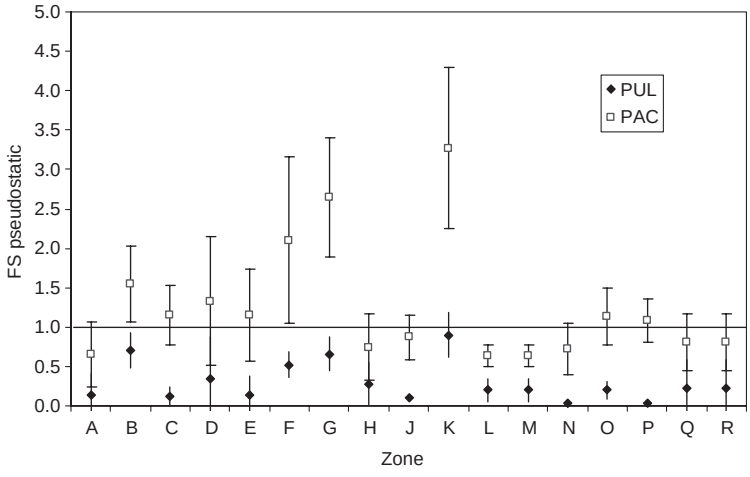

Fig. 7. Mean plus/minus one standard deviation (bars) values corresponding to the lowest pseudostatic factor of safety (FS) for potential block sliding failure modes at Pacoima Canyon, under ground shaking assumed equivalent to that recorded at the bottom of the canyon (PAC) and on top of a ridge (PUL).

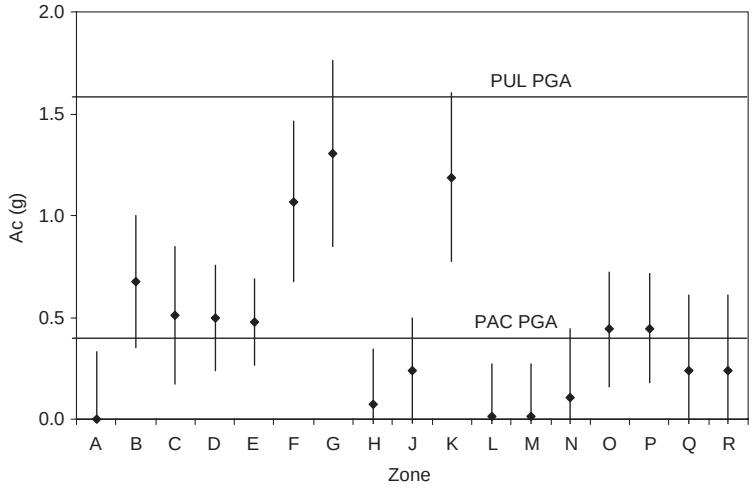

Fig. 8. Mean plus/minus one standard deviation (bars) values of the lowest critical acceleration for sliding (A_c) calculated for potential block sliding failure modes at Pacoima Canyon. Peak ground accelerations (PGA) at stations PAC and PUL are shown for comparison.

zones, between 10% and 50% for four zones, and over 80% for just four areas (Fig. 9). These results tend to confirm the observations from deterministic analyses, suggesting that even considering the high levels of uncertainty in the data, less than half of the zones would have shown slope failure.

4.3. Newmark-type analyses

The results of the pseudostatic analyses suggested that the landsliding would have been far less extensive than observed in the absence of topographic amplification. A second approach that would allow corroboration of these results is the use of Newmark (1965) analysis, based on an analogy of a rigid block sliding on an inclined plane. The analysis consists of the calculation of the cumulative permanent displacement of the sliding mass (called Newmark displacement) through double integration of the parts of the acceleration time history that exceed the critical acceleration defined in Eq. (2).

The analyses were performed using software for Newmark analyses developed by Jibson and Jibson (2003). Horizontal components records from the PAC

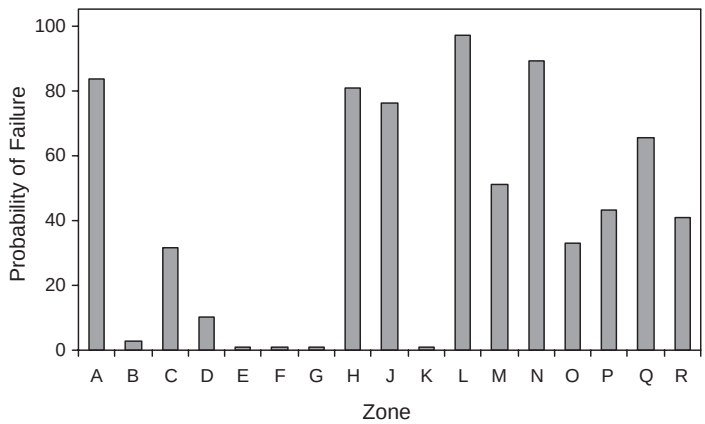

Fig. 9. Probability of failure at the area of study under normal (unamplified) seismic conditions (represented by records from station PAC) during the 1994 Northridge earthquake, considering planar and wedge failure modes.

and PUL stations having orientations closest to the slope dip direction were used. The resulting Newmark displacements (Fig. 10) can be compared with threshold displacements leading to significant strength reduction and likely catastrophic failure for rock falls and disrupted/non-cohesive slides. Such thresholds are normally about 2–5 cm (Wilson and Keefer, 1985; Wieczorek et al., 1985). Most of the slopes in the study area that produced landslides suffered catastrophic failure, with block sliding becoming rock falls, although some wedge failures with limited displacement were also reported in slopes supported by shotcrete (Harp and Jibson, 2002).

For unamplified ground motions (PAC record), only 5 of the 17 slopes analysed had displacements greater than 2 cm, and more than half the slopes had negligible displacements (Fig. 10). By contrast, analyses using amplified motions (PUL record) yield displacements greater than 2 cm for 13 of the 17 slopes and displacements greater than 5 cm for 12 of the slopes. Zones B, F, G and K yielded displacements below the threshold. The incidence of landsliding in these areas however, may be explained by the lack of consideration of potential toppling failure in these analyses. In zones G and K toppling was found to be an important failure mode in kinematic analyses. Additionally the omission of vertical accelerations (as discussed below) in the analyses may have been important in some cases.

These results support the conclusions from pseudostatic analyses that the unamplified motion was not strong enough to trigger the observed amount of landsliding. The low vertical acceleration recorded at PAC station is not likely to increase the displacements sufficiently to change this situation.

5. Discussion

Our results are consistent with those of Harp and Jibson (2002) that the much higher density of landslides at Pacoima Canyon compared with nearby canyons in the San Gabriel Mountains was a result of stronger ground shaking as a consequence of local topographic amplification rather than higher overall rock mass susceptibility. Similar observations are drawn from different types of limit equilibrium analyses, including probabilistic approaches that were used to test the reliability of the analytical method given the uncertainty in the geotechnical inputs, as well as Newmark-displacement analyses.

Our results and the landslide distribution suggest that topographic amplification occurred not only in the canyon downstream from the dam but also in some slopes surrounding the reservoir. Our analyses used amplified motion from the PUL station on the upper left abutment of the dam, a station that has repeatedly recorded abnormally high motions in recent earthquakes (Harp and Jibson, 2002). However, using this record for analysis does not suggest that the accelerations in all the slopes were equal to that recorded at PUL; variables such as slope orientation,

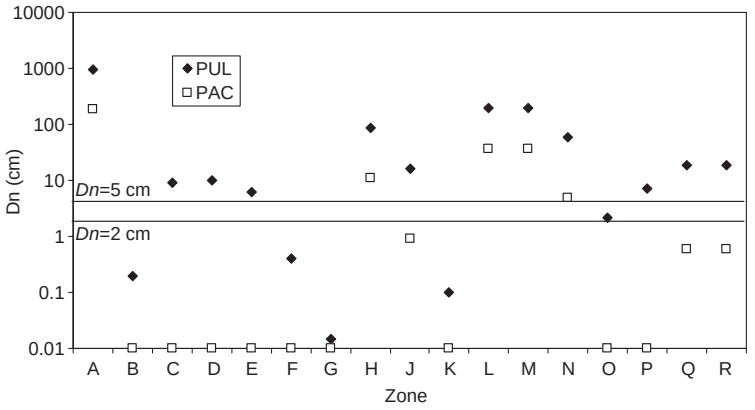

Fig. 10. Newmark displacements (Dn) for the investigated areas using horizontal seismic records from PAC and PUL stations. Displacements of 0.01 cm in the chart should be considered to indicate zero movement.

slope angle and in some extent lithology influence the amount of amplification (Geli et al., 1988; Ashford and Sitar, 1997; Ashford et al., 1997). Nevertheless, values of critical acceleration for sliding and Newmark displacement analyses suggest that accelerations around and over 1.0 g would have occurred in several slopes in the study area.

The Newmark analysis as used in this study ignores vertical accelerations. Recent research has shown, however, that vertical accelerations can have a significant effect on slope performance (Huang et al., 2001). The omission of vertical accelerations may yield lower bound displacements from the analyses, particularly for PUL records for which the vertical acceleration was large. In such cases, vertical accelerations may have a significant impact on slope stability by affecting the shear and normal stresses on sliding blocks with steep shear surfaces and by a loosening effect on the block interlocking, inducing larger displacements than those calculated omitting vertical motions.

Kinematic analyses correctly identify the susceptibility of slopes to earthquake-induced landsliding in different zones, compared to field observation. However, given the uncertainty in ground motion amplitude, and potential rate-dependent effect on the frictional shear strength of discontinuities (Crawford and Curran, 1981; Hencher, 1981), such results should be treated as susceptibility only and supplemented by more rigorous slope stability analyses for the assessment of the seismic response of slopes.

Finally, the results clearly demonstrate the need for careful consideration of input ground motion for seismic slope stability analysis. The nature of the problem is such that the slopes most prone to topographic amplification are those that are probably most prone to failure, given similar rock mass quality and kinematic susceptibility. Therefore, the results show the importance of considering topographic amplification effects on hazard assessment of earthquake-triggered landslides.

6. Summary and conclusions

Analysis of the stability conditions of the rock slopes at Pacoima Canyon show that the failures triggered by the 1994 Northridge earthquake were controlled principally by two factors: the orientation of discontinuities and topographic amplification of the strong motion. Discontinuity orientation facilitated both planar and wedge sliding of masses out of the rock face. Both pseudostatic (deterministic and probabilistic) and Newmark-type stability analyses indicated that the unamplified strong motion recorded at the bottom of the canyon (station PAC), similar to records in surrounding areas, would have been not strong enough to trigger the large number of failures observed in 1994. According to the analyses, under unamplified conditions landslides would have been triggered in about half of the zones actually affected by failures. In contrast, analyses using the amplified record from the left dam abutment ridge (station PUL) show that the amplified strong motion would explain the high landslide density and distribution at the site compared to surrounding areas.

This study reveals the importance of considering site effects such as topographic amplification on hazard assessment of seismically induced landslides.

Acknowledgements

The Los Angeles Department of Public Works kindly provided access to the study area. We particularly thank Robert Larson and the staff at the site office at Pacoima Reservoir for their assistance in the development of the field work. The study is part of a project funded by the Universities of Leeds, Durham, and Chile, the Chilean government, and the Geological Society of America.

References

Anooshehpoor, A., Brune, J.N., 1989. Foam rubber modeling of topographic and dam interaction effects at Pacoima dam. Bulletin of the Seismological Society of America 79 (5), 1347–1360.

Ashford, S., Sitar, N., 1997. Analysis of topographic amplification of inclined shear waves in a steep coastal bluff. Bulletin of the Seismological Society of America 87 (3), 692–700.

Ashford, S., Sitar, N., Lysmer, J., Deng, N., 1997. Topographic effects on the seismic response of steep slopes. Bulletin of the Seismological Society of America 87 (3), 701–709.

Barton, N., 1976. The shear strength of rock and rock joints. International Journal of Rock Mechanics and Mining Sciences and Geomechanics Abstracts 13, 255–279.

Boore, D.M., 1972. A note on the effect of simple topography on seismic SH waves. Bulletin of the Seismological Society of America 62 (1), 275–284.

Boore, D.M., 1973. The effect of simple topography on seismic waves: implications for the accelerations recorded at Pacoima Dam, San Fernando Valley, California. Bulletin of the Seismological Society of America 63 (5), 1603–1609.

Bouchon, M., 1973. Effect of topography on surface motion. Bulletin of the Seismological Society of America 63 (2), 615–632.

Chang, S.W., Bray, J.D., Seed, R.B., 1996. Engineering implications of ground motions from the Northridge earthquake. Bulletin of the Seismological Society of America 86 (1B), S270–S288.

Crawford, A.M., Curran, J.H., 1981. The influence of shear velocity on the frictional resistance of rock discontinuities. International Journal of Rock Mechanics and Mining Sciences and Geomechanics Abstracts 18, 505–515.

Geli, L., Bard, P.Y., Jullien, B., 1988. The effects of topography on earthquake ground motion. A review and new results. Bulletin of the Seismological Society of America 78 (1), 42–63.

Harp, E.L., Jibson, R.W., 1996. Landslides triggered by the 1994 Northridge, California, earthquake. Bulletin of the Seismological Society of America 86 (1B), S319–S332.

Harp, E.L., Jibson, R.W., 2002. Anomalous concentrations of seismically triggered rock falls in Pacoima Canyon: are they caused by highly susceptible slopes or local amplification of seismic shaking? Bulletin of the Seismological Society of America 92 (8), 3180–3189.

Harp, E.L., Noble, M.A., 1993. An engineering rock classification to evaluate seismic rock-fall susceptibility and its implication to the Wasatch Front. Bulletin of the Association of Engineering Geologists 30, 293–319.

Hatzor, Y.H., Goodman, R.E., 1997. Three-dimensional back-analysis of saturated rock slopes in discontinuous rock — a case study. Geotechnique 47 (4), 817–839.

Hencher, S.R., 1981. Friction parameters for the design of rock slopes to withstand earthquake loading. Dams and Earthquake. Thomas Telford Ltd., London, pp. 79–87.

Hoek, E., 2000. Practical Rock Engineering. [Online] Rocscience. Available from World Wide Web http://www.rocscience.com/hoek/PracticalRockEngineering.asp.

Hoek, E., Bray, J.W., 1981. Rock Slope Engineering, 3rd edition. Institution of Mining and Metallurgy, London.

Huang, C.C., Lee, Y.H., Liu, H.P., Keefer, D.K., Jibson, R.W., 2001. Influence of surface-normal ground acceleration on the initiation of the Jih-Feng-Erh-Shan landslide during the 1999 Chi-Chi, Taiwan, earthquake. Bulletin of the Seismological Society of America 91 (5), 953–958.

Jibson, R.W., Jibson, M.W., 2003. Java Programs for Using Newmark's Method and Simplified Decoupled Analysis to Model Slope Performance During Earthquakes, Version 1.1. [CD-Rom]. U.S. Geological Survey, Open-File Report 03-005.

Kramer, S.L., 1996. Geotechnical Earthquake Engineering. Prentice-Hall, Upper Saddle River.

Newmark, N., 1965. Effects of earthquakes on dams and embankments. Geotechnique 15 (2), 139–160.

Palisade Corporation, 2002. Guide to Using @Risk, Risk Analysis and Simulation Add-Inn for Microsoft Excel, Version 4.5.

PEER, 2000. Strong Motion Database, Pacific Earthquake Engineering Research Center. Available in the World Wide Web http://peer.berkeley.edu/smcat.

Sepúlveda, S.A., Murphy, W., Petley, D.N., 2005. Topographic controls on coseismic rock slides during the 1999 Chi-Chi earthquake, Taiwan. Quarterly Journal of Engineering Geology and Hydrogeology 38 (2), 189–196.

Spudich, P.S., Hellweg, M., Lee, W.H.K., 1996. Directional topographic site response at Tarzana observed in aftershocks of the 1994 Northridge, California, earthquake: implications for mainshock motions. Bulletin of the Seismological Society of America 86 (1B), S193–S208.

Vahdani, S., Wikstrom, S., 2002. Response of the Tarzana strong motion site during the 1994 Northridge earthquake. Soil Dynamics and Earthquake Engineering 22, 837–848.

Wieczorek, G.F., Wilson, R.C., Harp, E.L., 1985. Map Showing Slope Stability During Earthquakes in San Mateo County, California. U.S. Geological Survey Miscellaneous Investigation Maps I-1257-E.

Wilson, R.C., Keefer, D.K., 1985. Predicting areal limits of earthquake-induced landsliding. In: Ziony, J.I. (Ed.), Evaluating Earthquake Hazards in Los Angeles Region — An Earth Science Perspective, U.S. Geological Survey Professional Paper, vol. 1360.

Wong, H.L., Jennings, P.C., 1975. Effects of canyon topography on strong ground motion. Bulletin of the Seismological Society of America 65 (5), 1239–1257.

Yerkes, R.F., 1996. Preliminary Geologic Map of the San Fernando 7.5' Quadrangle, Southern California. U.S. Geological Survey, Open-File Report 96-88.